

1

Fundamental Understandings of Superamphiphobicity

Hui Liu¹, Qing Xu¹, Chengyuan Zhang¹, Jianying Huang², and Yuekun Lai^{2,3*}

¹National & Local Joint Engineering Research Center of Technical Fiber Composites for Safety and Health, School of Textile & Clothing, Nantong University, Nantong 226019, People's Republic of China

²National Engineering Research Center of Chemical Fertilizer Catalyst (NERC-CFC), College of Chemical Engineering, Fuzhou 350116, People's Republic of China

³Qingyuan Innovation Laboratory, Quanzhou 362801, People's Republic of China

*Corresponding author: yklai@fzu.edu.cn

1.1 Natural Creatures with Special Wettability

In order to acclimatize themselves to the natural environment, many plants and animals in nature have developed particular morphology and structures during long-time evolution. Recent advances in comprehending the underlying mechanisms of naturally occurring superhydrophobic and superoleophobic surfaces have prompted an abundance of biomimetic studies modeled after the characteristics of gecko setae, butterfly wings, and other structures [1, 2]. Particular attention has been paid to a number of well-known instances of oil-repellent surfaces found in nature (in the air) [3]. For example, bacterial (*Bacillus subtilis*) biofilm colonies and pellicles (Figure 1.1a) have a persistent antiwetting property to many liquids with low surface tension, as reported by Nishimoto et al. [4]. According to Gorb's group, leafhoppers with consistent and dense coatings of bronchosomes, a type of highly organized particle, were oil-repellent on their integuments (Figure 1.1b) [5]. Werner et al. discovered that springtails (also known as collembolan), as one of the most significant and attractive natural organisms with oil repellency, can sustain themselves without suffocating in water or even oil environments [6–9]. The cuticle structures of these organisms display robust surface plasmons that are made up of hexagonal or rhombic comb-like patterns or secondary granules with hexagonal basic patterns. A visible layer of protective air cushion, characteristic of a superamphiphobic surface, was present on the surfaces after the springtails were submerged in water and oil. After conducting a thorough investigation into the cuticle micro- or nanomorphology of approximately 40 different springtail species (Figure 1.1c–f), the researchers concluded that the extreme oil repellency of these springtails in air is a result of a combination of multiscale roughness (e.g. the reentrant topography) and chemical composition

Superamphiphobic Surfaces: Fabrication, Characterization, and Applications, First Edition.

Edited by Junping Zhang and Mohammad Shahid.

© 2025 Wiley-VCH. Published 2025 by Wiley-VCH.

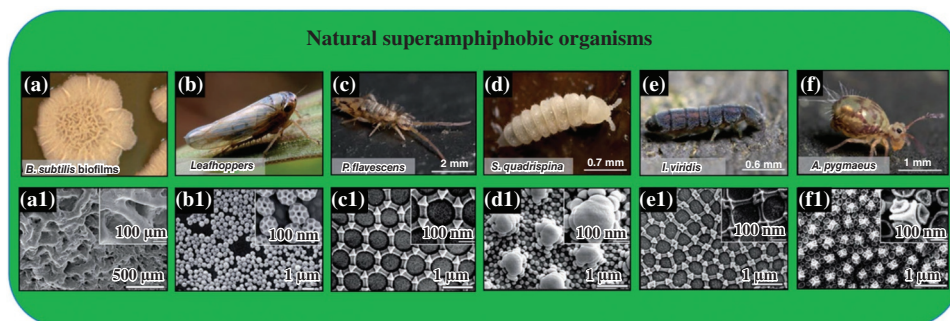


Figure 1.1 Habitus images and respective morphological characteristics of representative oil-repellent examples in nature. (a, a1) Bacterial biofilms of *Bacillus subtilis* [4] / National Academy of Sciences. (b, b1) Leafhoppers [5] / Royal Society Publishing. (c–f) Different species of springtails [8] / Springer Nature.

(e.g. chitin or protein). The inspiration from these oleophobic surfaces in nature has paved the way for more examples of oil-repellent surfaces [10–12].

1.2 Characterization of Wettability

A sessile drop will normally form in the shape of a sphere sectioned by the surface when it is placed on a flat substrate. There is a discrete and measurable contact angle θ_{CA} between the sphere and the surface at the circular solid–liquid–vapor three-phase contact line. Generally speaking, a hydrophilic surface possesses $\theta_{CA} < 90^\circ$, while hydrophobicity displays $\theta_{CA} > 90^\circ$. A surface is specifically designated as super-repellent if its θ_{CA} is greater than 150° and its sliding angle θ_{SA} is less than 10° . Superhydrophobicity refers to a surface that exclusively repels water, while superamphiphobicity is the ability of a surface to exhibit super-antiwetting properties toward both water and other oil liquids with surface energy lower than water. Characterization is crucial in order to explore the superamphiphobic characteristics. The most straightforward method for locating a super-antiwetting surface is usually eye visualization. Using this technique, the wetting and flowing behaviors can be observed when a probing liquid is applied gently to the surface. If oils and water can both flow across the surface easily, it is considered superamphiphobic. However, precise professional equipment is required to measure the static contact angle and contact angle hysteresis in order to accurately distinguish between various super-repellent properties.

1.2.1 Static Contact Angle

Classically, the static contact angle, as given by Young's equation (Figure 1.2a), is the traditional method used to determine the surface wettability. When a droplet of fluid comes into contact with a surface, a combination of interfacial tensions between the solid–liquid (γ_{SL}), solid–vapor (γ_{SV}) and liquid–vapor (γ_{LV}) interfaces can control the contact angle:

$$\cos \theta_{CA} = \frac{\gamma_{SL} - \gamma_{SV}}{\gamma_{LV}} \quad (1.1)$$

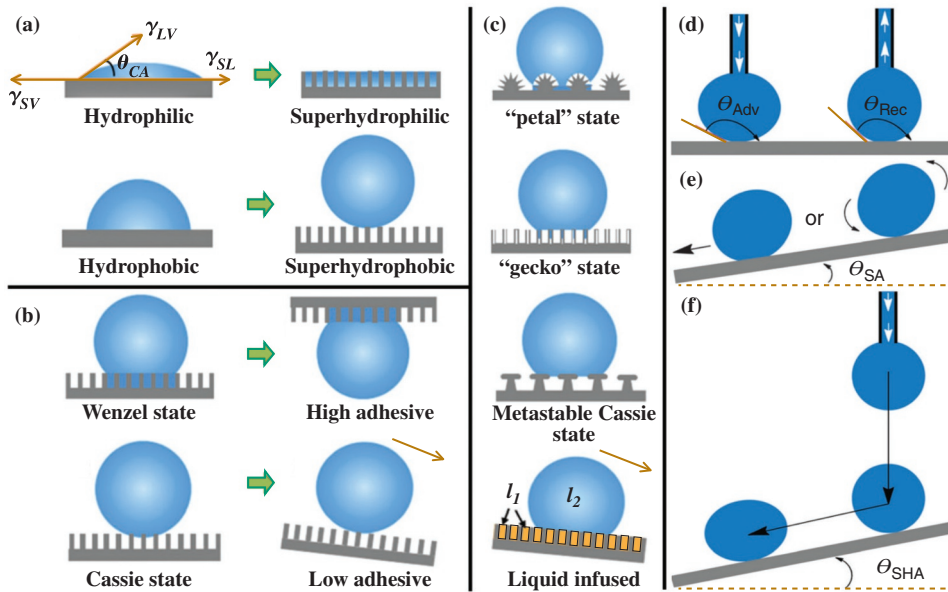


Figure 1.2 (a) Rough structures can enhance surface wettability. (b) The droplet with high adhesive force in the Wenzel state can firmly adhere to the substrate surface even when it is reversed downwards. The droplet with low adhesive force in Cassie state can easily roll down the substrate. (c) Several typical states of super-repellant surfaces: “petal” state; “gecko” state; metastable Cassie state; and liquid-infused state [25]. Schematic illustration of the characterization analysis for contact angle hysteresis [26]: (d) advancing θ_{Adv} and receding contact angle θ_{Rec} ; tilt angle, i.e. the so-called roll-off angle or sliding angle θ_{SA} (e) and the shedding angle θ_{SHA} (f).

However, the aforementioned Young’s equation [13] only can be applied to smooth, flat surfaces, ignoring the actual interactions between droplets and substrates as well as other external forces in practical situations [14]. But in fact, such an ideal surface does not exist. Due to the more complex solid–liquid interactions, contact angles on a rough surface typically exhibit fluctuation. Two distinct models have been constructed to represent the water contact in the Cassie–Baxter regime [15] and the Wenzel regime [16] in order to better explain this phenomenon. In the Wenzel regime, surface roughness can promote both wettability and nonwettability, depending on the surface’s chemical properties (Figure 1.2a,b). In this regime, the following equation [17] describes the relationship between the measured θ_{CA} and the “true” contact angle of a flat surface (θ_{flat}):

$$\cos \theta_{CA} = R \cdot \cos \theta_{flat} \quad (1.2)$$

where R is the ratio of the actual surface area of the rough surface to the apparent area.

A composite liquid–vapor–solid interface and a more antiwetting surface might result from stable air pockets existing in rough interstices between the droplets and surfaces. This situation is known as the Cassie–Baxter regime [17].

$$\cos \theta_{CA} = -1 + \varnothing_S \cdot (1 + \cos \theta_{flat}) \quad (1.3)$$

where \varnothing_S is the fraction of the surface that is in contact with the liquid. In this condition, the liquid just partially rests on the surface, with a relatively tiny contact area. Because of

the trapped air in the pores, the contact angles of a rough surface composed of the same materials are always significantly larger than those of a flat surface. Consequently, surface morphology plays a very key role in wettability.

The two states described above are always considered as extreme cases where droplets are positioned on extremely repellent surfaces. However, in certain exceptional circumstances, certain intermediate states, such as the “petal” state [18], “gecko” state [19], and metastable Cassie state [20], also occur, where droplets may partially moisten the roughened surfaces (Figure 1.2c). The droplet partially wets the surface of a rose petal as it penetrates into the rough structure. The large-scale micropapillae on the petal surface are shown to be impregnated by droplets, but the nanofolds that sit on top of them remain unwetted. Even when the petals are positioned upside down in this wetting case, the droplets are still able to adhere firmly to their surfaces. Additionally, a different high-adhesion wetting condition known as the “gecko” state explains a negative pressure created by sealed air pockets trapped in the nanospace between the surface and the water droplet, which results in a high adhesive force. As implied by its name, the metastable Cassie state is not an actual equilibrium state. Such a state originates from a superoleophobic surface with local curvature. Despite having low surface tension and liquid CA greater than 90° , the textured surface’s air–liquid interface is pinned by the local surface curvature, which keeps the liquid from penetrating and giving rise to the superoleophobic property [21–24]. Nevertheless, the surface may lose its superoleophobicity if some external disturbance causes it to transition from the metastable Cassie state to the Wenzel state.

It is noteworthy that the liquid-infused surface has been recently developed into a liquid-repelling one. Its repellency, however, cannot be explained by the Wenzel and Cassie–Baxter equations. Rather, instead of using micro/nanoscale features to reject fluids, the liquid-infused surface has eliminated adhesion between the droplet and the substrate depending on the liquid surface. The oil liquids with extremely low surface energy can produce a stable and smooth interface, restricting most liquids from permeating and at the same time resisting the adhesion of a variety of matters [25].

1.2.2 Contact Angle Hysteresis

Not only must the contact angle for water and oil droplets be greater than 150° , but a comparable low contact angle hysteresis (CAH) is also necessary for a super-repellent surface. The difference between two contact angles, viz. advancing contact angle (Adv) and the receding contact angle (Rec) on a surface with a specific roughness or uneven chemical composition is known as the CAH [14]. CAH has an impact on surface adhesion. For example, a self-cleaning surface requires a low hysteresis. Thus, for superhydrophobic and superoleophobic surfaces, CAH is yet another crucial character. Many methods have been devised to date for the characterization of the CAH; the most commonly used ones are $\theta_{Adv}/\theta_{Rec}$ and the tilt angle.

Advancing/receding contact angle: Usually, the advancing contact angle (θ_{Adv}) and the receding contact angle (θ_{Rec}) are typically measured using commercial equipment equipped with an enhanced video microscopy system and digital image analysis (Figure 1.2d). First, a syringe pump is applied to generate a standard water droplet. And then the water fluid is continuously pumped into (or sucked from) the droplet at a lower speed. In the meantime,

a solid state charge-coupled device camera displays θ_{Adv} in a frame grabber. Following the water pumping, the suction action is carried out to recede the water droplet, and to record the θ_{Rec} [27].

Tilt angle: A critical angle between the substrate and the horizontal surface is termed as the tilt angle, below which the droplet starts to move upon inclining the substrate. For both water and oil droplets, a tilt angle smaller than 10° is thought to be required for the super-repellent surfaces and self-cleaning properties. The two types of tilt angles that are typically distinguished are the sliding angle (θ_{SA} ; Figure 1.2e) and the shedding angle (θ_{SHA} ; Figure 1.2f). When a droplet fully rolls off the surface due to gravity alone, the angle of inclination of the surface is known as the sliding angle, also known as the roll-off angle. The sliding angle can be measured by the θ_{CA} measuring instrument through the use of a tilt plate with an angle that can be adjusted between 0° and 90° . The plate rotates continuously from 0° to 90° during the measuring procedure until the droplet begins to roll or slide off the substrate surface [22, 28]. The rotation angle is immediately noted as θ_{SA} . There is, in fact, a small difference between sliding and rolling with respect to the droplet's real motion. The sliding case has a somewhat bigger contact area between the droplet and the substrate than the rolling case. Furthermore, in the former case, the droplet gets stuck on the substrate because of the strong adhesive force, whereas in the latter case, the droplet is free to roll [29–31]. Nevertheless, in most of the cases, the difference was not reported along with the recorded angle. The sliding angle approach is no longer suitable when measuring surface adhesion on some difficult surfaces, including textiles, because of the many clinging fibers that obstruct droplet sliding [28]. Consequently, a new method called the shedding angle has been proposed for the characterization of superhydrophobic textiles [32]. In essence, the shedding angle (θ_{SHA}) is a critical angle at which a water droplet of a certain volume dropped from a set height begins to roll off or bounce away from the inclined substrate. When comparing data from several studies, caution must be taken because the drop volume and needle-to-substrate distance have an impact on the measured θ_{SHA} value.

1.3 The Mechanism for Superamphiphobicity

1.3.1 Chemical Composition

Owing to its decisive effect on surface energy, the chemical composition is a major factor in a material's wettability. Young's equation (Eq. 1.1) provides a good description of the CA of a flat substrate [13]. On a flat surface, hydrophobicity or oleophobicity must be achieved with a CA greater than 90° for both water and oil droplets. γ_{sv} is less than γ_{sl} if CA is more than 90° . Ignoring that the contact force between two surfaces has an actual order, Eq. (1.4) allows us to approximate the γ_{sl} [33]:

$$\gamma_{sl} = \gamma_{sv} + \gamma_{lv} - 2\sqrt{\gamma_{sv}\gamma_{lv}} \quad (1.4)$$

The surface free energy of the solid substrates (γ_{sv}) should be sufficiently low to be less than one-quarter of the surface free energy of the liquid (γ_{lv}), as determined by combining Eqs. (1.1) and (1.2). Some common oils, including hexadecane, have surface tensions that

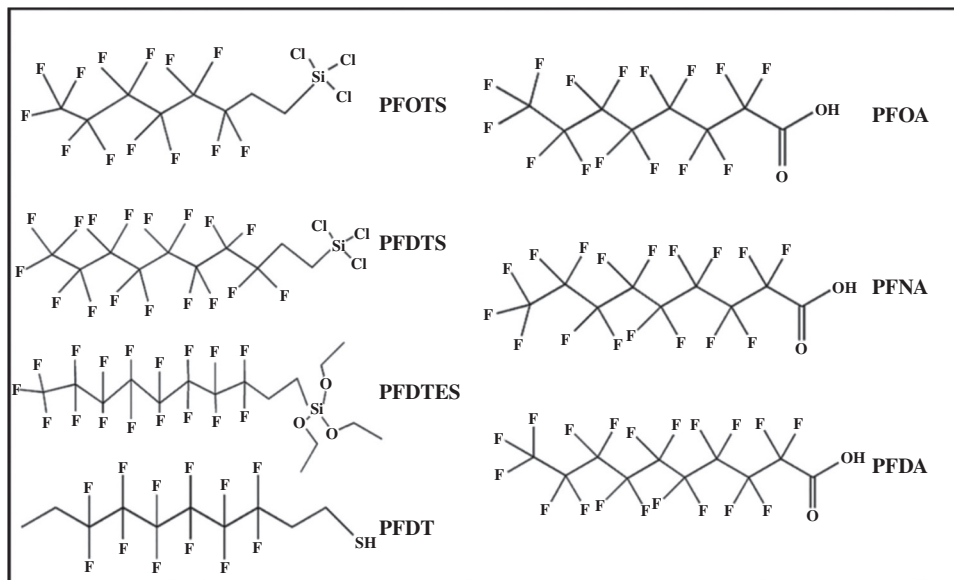


Figure 1.3 Chemical structures of commonly used perfluorinated materials applied to the surface modification of a roughened substrate.

are typically substantially lower than water's (27.5 m Nm^{-1}). Therefore, the solid surface's surface energy needs to be extremely low, just a few m Nm^{-1} , in order to achieve superoleophobicity. Only a few unique chemical groups, such as $-\text{CF}_3$, allow for this. This rigid requirement restricts the choice of materials and enhances the challenge of fabricating superamphiphobic surfaces.

Generally speaking, the appropriate materials can be created by depositing molecular perfluoroalkane that has a functional group at one terminal (F-monomer), such as 1H,1H,2H,2H-perfluorooctyl phosphate (PFOP), 1H,1H,2H,2H-perfluorooctanoic acid (PFOA), 1H,1H,2H,2H-perfluorooctyl trichlorosilane (PFOTS), 1H,1H,2H,2H-perfluorodecyl trichlorosilane (PFDTs), 1H,1H,2H,2H-perfluorodecane-1-thiol (PFDSH), and 1H,1H,2H,2H-perfluorodecyl acrylate (PFDAE). Additionally, it can also be achieved by spin- or spray-coating a solution of fluorinated polymers (F-polymers). F-monomers can always be grafted to create a fluorinated layer either liquid phase deposition or vapor phase deposition.

The fluorinated materials can be broadly classified into the following groups based on the types of chemical modification materials: fluoroalkane, perfluorocarboxylic acid, fluoropolymers, fluorosurfactants as well as C_4F_8 plasma. Figure 1.3 summarizes a few perfluorinated compounds that are often utilized. This section will cover the benefits and drawbacks of each fluorinated material.

1.3.1.1 Fluoroalkane

Fluoroalkanes are frequently utilized for prepatterned surfaces and are thought to be the ideal compounds to make superamphiphobic surfaces. Generally, perfluoroalkane with a functional group at the chain terminal (F-monomer) can be deposited on a variety of

substrates to generate a fluorinated layer. Fluorosilanes and fluorothiols are the two types of fluoroalkanes that are frequently employed.

Fluorosilanes: On many different patterned substrates, fluorosilanes can produce thin, self-assembling layers. Before fluorination, the patterned surface must be activated (by UV or plasma) to form $-OH$ on the surface. After fluorosilanes are added, a covalently linked layer can be achieved. Fluorosilanes that are primarily used in applications are 1H,1H,2H,2H-perfluorooctyltrichlorosilane (PFOTS), 1H,1H,2H,2H-perfluorodecyltrichlorosilane (PFDTs), and 1H,1H,2H,2H-perfluorodecyltriethoxysilane (PFDTES). Wong et al. have fabricated transparent and superamphiphobic surfaces with inverted cone nanostructures by omnidirectional self-assembly of nanoparticle aerosols and gas phase fluoro-silanization of PFOTS [34]. Besides, using a simple molding technique and PFDTs modification, Jang et al. were able to successfully produce functional superamphiphobic polymer-based surfaces [35]. The molding template was composed of hierarchical structures with ratchet-like microscale structures and nanoscale spheres and an ultrathin-protecting layer for the repeated molding process.

Fluorothiols: The fluorothiols are efficient fluoroalkane modifiers to reduce the surface energy of reentrant structure, much like fluorosilane. Moreover, thiols are able to form a thin, self-assembling layer on the substrates. However, they lack oxidative stability and are restricted to specific substrates like copper, silver, gold, platinum, palladium, or palladium [36–38]. 1-Decane-thiol (DT), as one type of fluorine-free low surface tension material, is utilized to passivate the prepatterned surface. The surface energy of DT is higher than that of PFDT (1H,1H,2H,2H) due to the distinct functional groups in their chemical structures (DT possesses $-CH_3$, PFDT $-CF_3$) [38]. Using a two-step surface texturing procedure and surface fluorination with PFDT, Ou et al. created a superamphiphobic surface [38]. Superamphiphobicity of the surface could be restored with remodification with PFDT, demonstrating indirectly that PFDT desorption may be the cause of the deterioration.

1.3.1.2 Perfluorocarboxylic Acids

Perfluorocarboxylic acid has also been employed to reduce the reentrant structure's surface energy. It is often applied to the prepatterned surface, just like the fluoroalkane compounds. Perfluorooctanoic acid (PFOA) [39], perfluorononanoic acid (PFNA) [40], and perfluorodecanoic acid (PFDA) [41] are examples of perfluorocarboxylic acids that are often used. Chen et al. [39] have developed a strong and long-lasting superamphiphobic surface with great repellency to various liquids, including water, glycerol, peanut oil, and some chemical solvents. The superamphiphobic powder's primary constituents were Cu and Cu_2O , which were covered in CF_3 and CF_2 functional groups. The superamphiphobic surface exhibited a high number of morphologies that resembled leaves, protrusions, and corallines, which randomly aggregated and were covered in a huge number of micro/nanoparticles.

1.3.1.3 Fluoropolymer

Another ideal low surface tension material for fluorinated modification is fluoropolymer. Usually, it mixes with nanoparticles, which are employed to produce superamphiphobicity by raising the surface roughness. The fluoropolymer's shortcomings include its inability to attain sufficient roughness on its own and its unsuitability for pretextured surfaces. That is

to say, more nanoparticles need to be introduced [42]. Furthermore, there is a need for additional improvement in the durability of the fluoropolymer-based superamphiphobic surface. Using SiO₂ nanoparticles and fluorinated polyurethane, Wang et al. created a superamphiphobic breathable membrane that was comparable to the process used to make amphiphobic nanofibrous membranes made of poly (trifluoroethyl methacrylate) and electrospun silica [42]. A three-step polymerization process with a terminal perfluoroalkane segment produced the fluorinated polyurethane.

1.3.1.4 Polyhedral Oligomeric Silsesquioxane

POSS, or polyhedral oligomeric silsesquioxane, is an organosilicon molecule that resembles a cage. It is surrounded by either 1H,1H,2H,2H-perfluorodecyl (FD-POSS) or 1H,1H,2H,2H-perfluorooctyl (FO-POSS). POSS has an ultralow surface tension, with a solid surface energy of about 11.5 mN m⁻¹ [43]. Pan et al. [43] created an electrospun layer of fluorodecyl POSS and cross-linked poly(dimethylsiloxane; PDMS) on top of the stainless steel wire meshes. For a variety of various polar and nonpolar low surface tension liquids, such as acids, alkalis, and solvents, the as-fabricated superamphiphobic surface exhibits a high contact angle (Figure 1.4c) due to a hierarchical structure (Figure 1.4a,b) and low surface energy. Crucially, the superamphiphobic surface demonstrates an efficient chemical shielding property and can chemically shield against nearly every type of liquid, whether organic or inorganic, polar or nonpolar, Newtonian or non-Newtonian (Figure 1.4d–f).

1.3.1.5 Fluorosurfactant

The superamphiphobic surface can also be effectively created using fluorosurfactant with a high surface energy head and a low surface energy tail group [42]. There could be a low surface energy barrier as a result of the fluorinated tails segregating at the surface. Using a wet-chemical technique, Zhou et al. produced a strong, self-healing, and superamphiphobic surface [44], which was created by dispersing fluorocarbon surfactant (DuPont Zonyl321), lyophobic nanoparticles (PTFE NPs), and fluorinated alkyl silane (FAS) in water. The goal of using PTFE NPs was to improve the surface's mechanical robustness and provide secondary roughness. FAS functioned as a coupling agent to enhance the adherence between the superamphiphobic coating on a variety of substrates, including fabrics, sponges, wood, glass, and metal, while also acting as a low surface tension modifier to lower the surface free energy by introducing a fluorinated alkyl chain (Figure 1.4g,h).

1.3.1.6 Plasma Treatment

Plasma treatment is an additional modifying technique. The octafluorocyclobutane (C₄F₈) plasma was used in this process to deposit a fluorocarbon film on the substrates. One benefit of the plasma treatment is that, regardless of its morphology, it can be administered to the entire surface [42]. However, due to unique experimental conditions and chemicals that place restrictions on the applications of plasma treatment, it is only applicable to small-scale treatments. Using soft lithographic microfabrication and C₄F₈ plasma treatment, Kang et al. created a strong superamphiphobic surface with mushroom-shaped micropillars [45]. Reentrant structures were produced using the direct micromolding technique (Figure 1.4i,j). Following the etching procedure, a thin and uniform polymeric layer was formed on the textured surface by introducing the C₄F₈ gas in a deep reactive ion

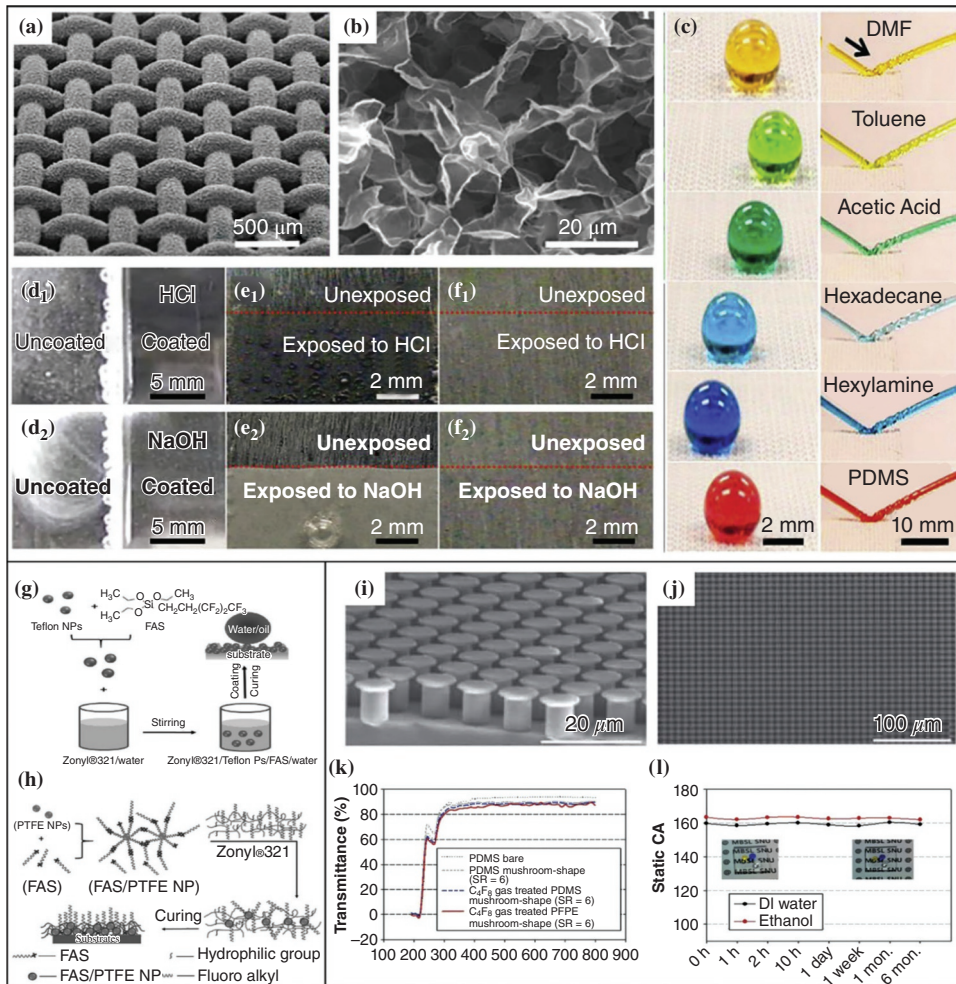


Figure 1.4 (a) SEM image of the hierarchically structured surface illustrating the electrospun coating of cross-linked PDMS +50 wt% fluorodecyl POSS on a stainless steel wire mesh 70. (b) SEM image illustrating the reentrant curvature of the electrospun texture. (c) Droplets of various low surface tension liquids showing very high contact angles. Side view of an aluminum plate, immersed in (d1) concentrated hydrochloric acid (HCl) and (d2) concentrated sodium hydroxide (NaOH), respectively. The uncoated aluminum surface reacts violently with HCl or NaOH, releasing bubbles of hydrogen gas, but the coated aluminum surface remains unaffected. The uncoated aluminum surface appears rough and damaged after immersion in (e1) HCl and (e2) NaOH, respectively. The coated aluminum surface remains unaffected after immersion in (f1) HCl or (f2) NaOH, respectively. (g) Schematic illustration of the procedure for solution preparation and coating treatment. (h) Illustration of possible interaction among PTFE NPs, FAS, and Zonyl321 [44]; (i, j) Side and top-view SEM images of PDMS mushroom-like micropillar arrays. (k) Transmittance spectra of various samples over UV-Vis wavelength regime. (l) Measurement of static contact angles of the PDMS sample over a time period of 6 months. The insets show optical photographs of various liquids: DI water (transparent), mineral oil (blue), and ethanol (yellow) at different time points [45] / with permission of The Royal Society of Chemistry.

etch system. In addition, C_4F_8 gas polymerization provides better resilience and repeatability when compared to alternative surface treatment techniques. Significantly, the polymer structures remain unchanged following the plasma treatment, which is thought to be a beneficial fluorocarbon surface treatment. As a consequence, the superamphiphobic surface is extremely repellent to different liquids with a broad range of surface tensions from 22.3 to 72.1 $mN\ m^{-1}$. The superamphiphobic surface has a transmittance of up to 90% (Figure 1.4k) and a durability of at least six months (Figure 1.4l).

1.3.2 Special Rough Morphology

The surface topology is another crucial factor. As previously mentioned, air can become trapped on a rough surface when liquids come into contact, significantly decreasing the contact between the surface and the droplet. However, repelling liquids with extremely low surface tension is not always the case for all rough surfaces with low surface energy. It was far from sufficient for industrial applications to repel just liquids with higher surface energy, such as water and glycol. To construct superoleophobicity, only a certain type of rough structure with reentrant geometries is applicable. In recent years, numerous review articles have concentrated on and gathered information about the design of complicated reentrant geometry, overhang structures, invertetrapezoidal structures, and mushroom-like structures, to fabricate superamphiphobic interfaces, as shown in Figure 1.5a–f [46–50]. The rough structure with reentrant curvature balances

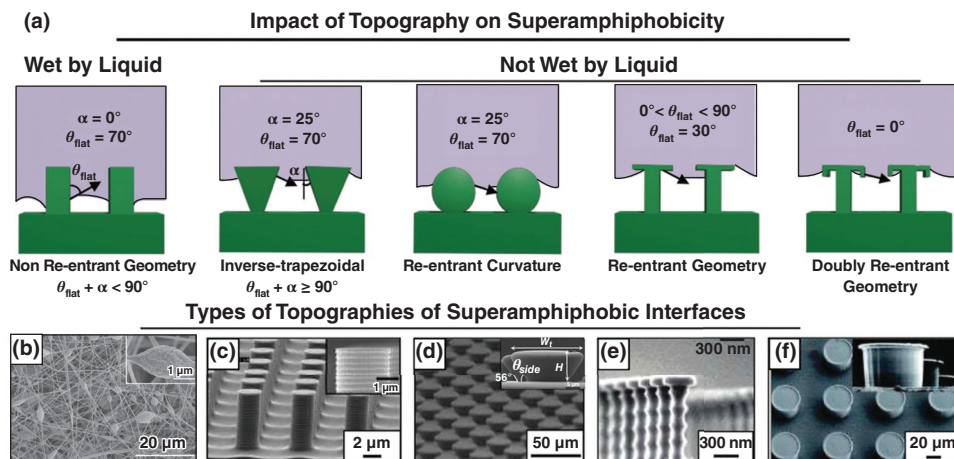


Figure 1.5 (a) Schematic depicting the impact of various reentrant topography for achieving superamphiphobicity. For non-reentrant geometry, the liquid wets the surface for $\theta_{flat} < 90^\circ$. When $\theta_{flat} + \alpha \geq 90^\circ$ for reentrant inverse trapezoidal geometry, the liquid does not wet the surface. But curvature geometry in reentrant structure supports the nonwetting of the surface with $\theta_{flat} = 70^\circ$. Also, other reentrant geometries support the nonwetting of the surface for $\theta_{flat} < 90^\circ$ and $\theta_{flat} = 0^\circ$ [46] / with permission of Elsevier. (b–f) SEM images of various reentrant geometries that aid in exhibiting superamphiphobicity including [51] / American Association for the Advancement of Science – AAAS (b) electrospun morphology, (c) well-defined micropillar type structures, (d) inverse trapezoidal microarrays, (e) wavy stem with wider head. (f) Overhang T-shaped microstructure [50] / The Royal Society of Chemistry.

the downward mixing force generated by Laplace pressure and droplet gravity and generates an upward combined force, therefore repelling liquids with lower surface tension.

1.3.2.1 Reentrant Structure

The notion of the reentrant surface structure was first proposed by Tuteja et al. [51] and used in the construction of superamphiphobic surfaces; it is thought to be an effective technique. Notably, this notion has significantly aided in the advancement of this field. So as to keep low contact angle hysteresis and reasonably high contact angles, superamphiphobic surfaces are predicted to produce composite solid–liquid–air interfaces with air pockets in the valleys between pillars. Reentrant curvature can be produced to some extent via mushroom-shaped structures, micro-hill-like structures, or even randomly stacked nanoparticles [52–55]. As we all know, the concave shape of the top of springtails, as one of the main factors, can contribute to liquid repellency. Kang et al. [52] used silicon microelectromechanical systems and soft lithography techniques to create mushroom-like micropillar (SIMM) arrays that resemble springtails in size and shape, with diminutive heads and broad feet. It was discovered that the meniscus of the SIMM array may be altered to provide selective liquid sliding features by varying the texturing angle and spacing between neighboring microcolumns. This occurs as a result of competition between internal gravity and Laplace pressure near the meniscus. It was shown that the mushroom-like head possesses both superomniphobicity and selective liquid sliding features. Zhang et al. [53] developed superamphiphobic surfaces with micro-hill-like reentrant microstructures by spraying fluorinated multiwalled carbon nanotubes (F-MWCNTs). The F-MWCNTs accumulating randomly and solvent evaporating jointly contributed to this particular reentrant structure. Such surface possesses sliding angles of 1.2° and 4.3° and contact angles of 172.4° and 163.0° for water and cetane, respectively (Figure 1.6a).

1.3.2.2 Overhang Structure

Previous research [56, 57] has indicated that innately hydrophilic materials can be made to exhibit superhydrophobic behavior if they have surfaces with microtextures with overhanging structures. These features contribute to keep water from entering grooves due to capillary forces. Likewise, it has been shown that superoleophobic surfaces can be formed on innately oleophilic substrates with overhang structures preventing oil from penetrating the textures, thus exhibiting superamphiphobicity [58–60]. Wang et al. [59] have developed a multifunctional coating composed of fluorinated alkyl silane, micro-sized ammonium polyphosphate particles, and functionalized silica nanoparticles (Figure 1.6b,c). A unique randomly overhanging hierarchical structure can be constructed on a variety of surfaces using an easy and economical spaying technique and exhibits super-repellency to water and oils with low surface tensions. Reverse imprint lithography and reactive ion etching techniques were used by Wooh et al. [60] to develop superamphiphobic surfaces with overhang patterns. They also incorporated conical, pillar, hole, and linear nanopatterns onto the overhang structure's surface in addition to the single overhang structure. The superoleophobicity of embedded holes and linearity could be enhanced by creating a new overhang angle of approximately 0° beside the original overhang structure, while the embedded conical and pillar nanopatterns just decrease the solid–liquid contact area.

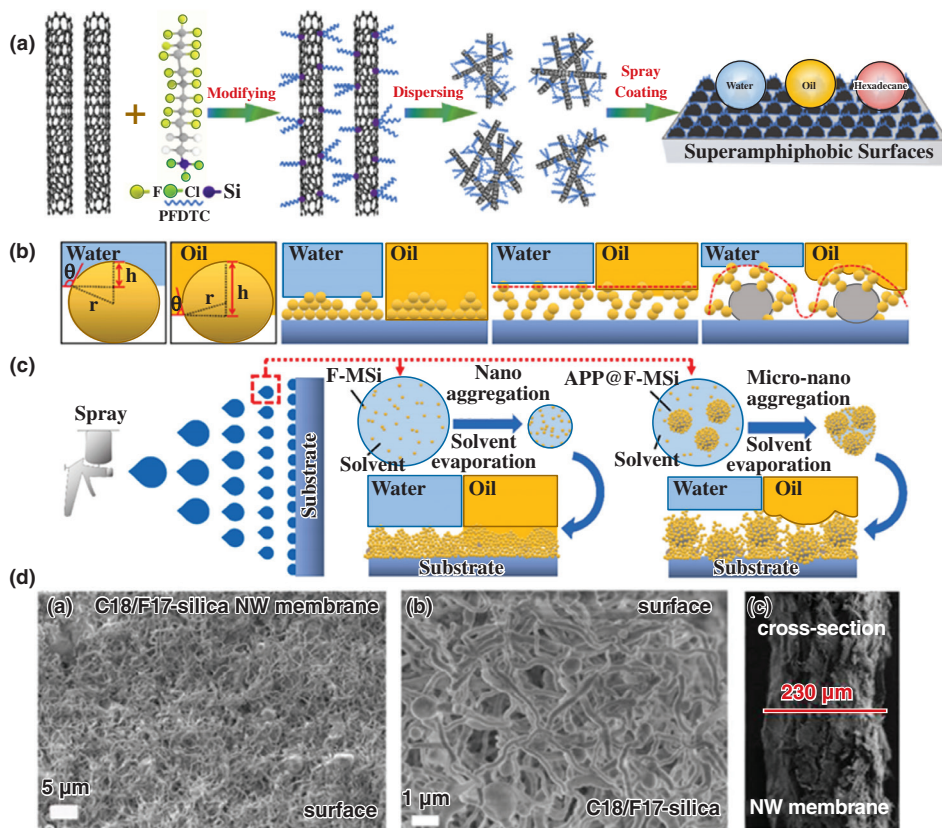


Figure 1.6 (a) Schematic illustration of the process for F-MWCNTs coating preparation [53] / with permission of Elsevier. (b) Schematic illustration of liquid-wetting models of a single particle with the radius r wetted by water and hexadecane. (h : penetration depth of the liquids; θ : the static contact angle of the liquids on a smooth surface possessing identical surface chemistry as the rough surface.) Assumed wetting models for the coating surfaces wetted by water and oil. (c) Schematic illustration of the mechanism of forming the superamphiphobic surface [59] / with permission of Elsevier. (d) General surface SEM, enlarged surface SEM, and cross-section SEM [62] / The Royal Society of Chemistry.

1.3.2.3 Porous Structures

Superamphiphobic coatings with porous structures are rarely constructed because of the unclear correlation between the structural parameters of the pores and the repellency of the coating. Nevertheless, it is worth noting that creating air pockets by trapping gas is crucial for liquid repellency as it creates negative Laplace pressure. Liquid repellency is greatly influenced by the amount of air present in the pores or vacancies of porous structures, another important type of nanostructure for creating superamphiphobic surfaces (Figure 1.6d) [61–63]. An artificial porous superamphiphobic surface has been developed by Li et al. [61] by combining adhesive agent polydopamine with hydrophilic SiO_2 nanoparticles for constructing a porous micro-network. Following a two-step CVD process, the superhydrophilic microstructure porous coating transformed into a superamphiphobic one. It should be highlighted that a porous coating's repellency is significantly influenced

by structural factors like pore height and size. Therefore, it is advantageous to optimize the structural characteristics in order to improve the coating's repellency. Besides, Cao et al. [63] have constructed a superamphiphobic, self-cleaning, and robust coatings on a variety of rock substrates depending on the low surface energy of fluorinated compounds and the inherent roughness of stone substrates. The superamphiphobic chemicals are housed in the pores of the stone, which functions as a microstructure to resist abradant removal and maintain the substrate's chemical and physical integrity.

Generally speaking, the two aforementioned factors should be carefully and extensively considered in order to properly accomplish superamphiphobicity.

1.4 Summary and Outlook

This section briefly introduced the several fundamental wetting states, dimensionless parameters, and design criteria that characterize the performance of a well-defined structured surface. Furthermore, commonly used chemical modification materials and a wide diversity of surface topographies of oil-resistant materials were summarized using pertinent classification.

To fully comprehend the superamphiphobic surface, it is important to discuss both current challenges and promising prospects. Firstly, additional investigation is needed to better comprehend the formation concept of a superamphiphobic system. The fundamental theory plays a very important guiding role in the fabrication and applications of superamphiphobic surfaces. Secondly, in order to quantify the performance stability of the superamphiphobic surface and facilitate performance comparison, a set of predetermined standards should be established. Last but not least, long-chain fluoride, which is frequently employed to reduce surface tension during chemical modification, is poisonous and harmful to the environment. Since low surface energy chemistry is not required, double reentrant structures should be further studied to produce superamphiphobic surfaces, as this is thought to be a more environmentally friendly technique. Double reentrant configurations can be optimized and used to build superamphiphobic surfaces by controlling the structural angle of the structured surface.

Generally speaking, there is still a huge potential for the development of superamphiphobic surfaces. With consistent effort, scientists and engineers will propose more theoretical research based on unique results to further grasp superamphiphobicity. A promising future lies ahead for superamphiphobic surfaces because of their high commercialization value and potential, which is driving an increasing number of scientists and engineers to strive for superamphiphobic surfaces.

Acknowledgments

The authors thank the National Natural Science Foundation of China (52102105, 22075046, 22375047, and 22378068), Natural Science Funds for Distinguished Young Scholars of Fujian Province (2020J06038), Natural Science Foundation of Fujian Province (2022J01568), National Key Research and Development Program of China (2022YFB3804905, 2022YFB3804900, and 2019YFE0111200), and 111 Project (No. D17005).

References

- 1 Nishimoto, S. and Bhushan, B. (2013). Bioinspired self-cleaning surfaces with superhydrophobicity, superoleophobicity, and superhydrophilicity. *RSC Advance* 3 (3): 671–690.
- 2 Liu, K., Du, J., Wu, J. et al. (2012). Superhydrophobic gecko feet with high adhesive forces towards water and their bio-inspired materials. *Nanoscale* 4 (3): 768–772.
- 3 Darmanin, T. and Guittard, F. (2015). Superhydrophobic and superoleophobic properties in nature. *Materials Today* 18 (5): 273–285.
- 4 Epstein, A.K., Pokroy, B., Seminara, A. et al. (2011). Bacterial biofilm shows persistent resistance to liquid wetting and gas penetration. *Proceedings of the National Academy of Sciences* 108 (3): 995–1000.
- 5 Rakitov, R. and Gorb, S.N. (2013). Brochosomal coats turn leafhopper (Insecta, Hemiptera, Cicadellidae) integument to superhydrophobic state. *Proceedings of the Royal Society B: Biological Sciences* 280 (1752): 20122391.
- 6 Helbig, R., Nickerl, J., Neinhuis, C. et al. (2011). Smart skin patterns protect springtails. *PloS One* 6 (9): e25105.
- 7 Hensel, R., Helbig, R., Aland, S. et al. (2013). Wetting resistance at its topographical limit: the benefit of mushroom and serif T structures. *Langmuir* 29 (4): 1100–1112.
- 8 Nickerl, J., Helbig, R., Schulz, H.J. et al. (2013). Diversity and potential correlations to the function of Collembola cuticle structures. *Zoomorphology* 132 (2): 183–195.
- 9 Nickerl, J., Tsurkan, M., Hensel, R. et al. (2014). The multi-layered protective cuticle of Collembola: chemical analysis. *Journal of the Royal Society Interface* 11 (99): 20140619.
- 10 Liu, K., Tian, Y., and Jiang, L. (2013). Bio-inspired superoleophobic and smart materials: design, fabrication, and application. *Progress in Materials Science* 58 (4): 503–564.
- 11 Brown, P.S. and Bhushan, B. (2016). Durable, superoleophobic polymer-nanoparticle composite surfaces with re-entrant geometry via solvent-induced phase transformation. *Scientific Reports* 6 (1): 21048.
- 12 Hensel, R., Neinhuis, C., and Werner, C. (2016). The springtail cuticle is a blueprint for omniphobic surfaces. *Chemical Society Reviews* 45 (2): 323–341.
- 13 Young, T. (1805). An essay on the cohesion of fluids. *Philosophical Transactions of the Royal Society A – Journals* 95: 65–87.
- 14 Genzer, J. and Efimenko, K. (2006). Recent developments in superhydrophobic surfaces and their relevance to marine fouling: a review. *Biofouling* 22 (5): 339–360.
- 15 Wenzel, R.N. (1936) Resistance of solid surfaces to wetting by water. *Industrial and Engineering Chemistry* 28 (8): 988–994.
- 16 Cassie, A.B.D. and Baxter, S. (1944). Wettability of porous surfaces. *Transactions of the Faraday Society* 40: 546–551.
- 17 Pan, S., Kota, A.K., Mabry, J.M. et al. (2013). Superomniphobic surfaces for effective chemical shielding. *Journal of the American Chemical Society* 135 (2): 578–581.
- 18 Feng, L., Zhang, Y., Xi, J. et al. (2008). Petal effect: a superhydrophobic state with high adhesive force. *Langmuir* 24 (8): 4114–4119.
- 19 Jin, M., Feng, X., Feng, L. et al. (2005). Superhydrophobic aligned polystyrene nanotube films with high adhesive force. *Advanced Materials* 17 (16): 1977–1981.

- 20 Tuteja, A., Choi, W., Ma, M. et al. (2007). Designing superoleophobic surfaces. *Science* 318 (5856): 1618–1622.
- 21 Tuteja, A., Choi, W., Mabry, J.M. et al. (2008). Robust omniphobic surfaces. *Proceedings of the National Academy of Sciences* 105 (47): 18200–18205.
- 22 Zhang, J. and Seeger, S. (2011). Superoleophobic coatings with ultralow sliding angles based on silicone nanofilaments. *Angewandte Chemie-International Edition* 50 (29): 6652.
- 23 Pan, S., Kota, A.K., Mabry, J.M. et al. (2013). Superomniphobic surfaces for effective chemical shielding. *Journal of the American Chemical Society* 135 (2): 578–581.
- 24 Liu, T.L. and Kim, C.J.C. (2014). Turning a surface superrepellent even to completely wetting liquids. *Science* 346 (6213): 1096–1100.
- 25 Wang, S. (2007). Definition of superhydrophobic states. *Advanced Materials* 19 (21): 3423–3424.
- 26 Chu, Z. and Seeger, S. (2014). Superamphiphobic surfaces. *Chemical Society Reviews* 43 (8): 2784–2798.
- 27 Cho, K.H. and Chen, L.J. (2011). Fabrication of sticky and slippery superhydrophobic surfaces via spin-coating silica nanoparticles onto flat/patterned substrates. *Nanotechnology* 22 (44): 445706.
- 28 Artus, G.R., Jung, S., Zimmermann, J. et al. (2006). Silicone nanofilaments and their application as superhydrophobic coatings. *Advanced Materials* 18 (20): 2758–2762.
- 29 Wong, T.S., Kang, S.H., Tang, S.K. et al. (2011). Bioinspired self-repairing slippery surfaces with pressure-stable omniphobicity. *Nature* 477 (7365): 443–447.
- 30 Huang, Y., Zhou, J., Su, B. et al. (2012). Colloidal photonic crystals with narrow stopbands assembled from low-adhesive superhydrophobic substrates. *Journal of the American Chemical Society* 134 (41): 17053–17058.
- 31 Mehanna, Y.A., Sadler, E., Upton, R.L. et al. (2021). The challenges, achievements, and applications of submersible superhydrophobic materials. *Chemical Society Reviews* 50 (11): 6569–6612.
- 32 Zimmermann, J., Seeger, S., and Reifler, F.A. (2009). Water shedding angle: a new technique to evaluate the water-repellent properties of superhydrophobic surfaces. *Textile Research Journal* 79 (17): 1565–1570.
- 33 Brown, P.S. and Bhushan, B. (2016). Durable, superoleophobic polymer–nanoparticle composite surfaces with re-entrant geometry via solvent-induced phase transformation. *Scientific Reports* 6 (1): 21048.
- 34 Wong, W.S., Liu, G., Nasiri, N. et al. (2017). Omnidirectional self-assembly of transparent superoleophobic nanotextures. *ACS Nano* 11 (1): 587–596.
- 35 Jang, H., Lee, H.S., Lee, K.S. et al. (2017). Facile fabrication of superomniphobic polymer hierarchical structures for directional droplet movement. *ACS Applied Materials and Interfaces* 9 (11): 9213–9220.
- 36 Zhu, X., Zhang, Z., Xu, X. et al. (2011). Rapid control of switchable oil wettability and adhesion on the copper substrate. *Langmuir* 27 (23): 14508–14513.
- 37 Lee, M.T., Hsueh, C.C., Freund, M.S. et al. (1998). Air oxidation of self-assembled monolayers on polycrystalline gold: the role of the gold substrate. *Langmuir* 14 (22): 6419–6423.

- 38 Ou, J., Hu, W., Liu, S. et al. (2013). Superoleophobic textured copper surfaces fabricated by chemical etching/oxidation and surface fluorination. *ACS Applied Materials and Interfaces* 5 (20): 10035–10041.
- 39 Chen, F., Song, J., Lu, Y. et al. (2015). Creating robust superamphiphobic coatings for both hard and soft materials. *Journal of Materials Chemistry A* 3 (42): 20999–21008.
- 40 Xu, Z., Zhao, Y., Wang, H. et al. (2015). A superamphiphobic coating with an ammonia-triggered transition to superhydrophilic and superoleophobic for oil-water separation. *Angewandte Chemie International Edition* 54 (15): 4527–4530.
- 41 Meng, H., Wang, S., Xi, J. et al. (2008). Facile means of preparing superamphiphobic surfaces on common engineering metals. *Journal of Physical Chemistry C* 112 (30): 11454–11458.
- 42 Wang, J., Raza, A., Si, Y. et al. (2012). Synthesis of superamphiphobic breathable membranes utilizing SiO₂ nanoparticles decorated fluorinated polyurethane nanofibers. *Nanoscale* 4 (23): 7549–7556.
- 43 Pan, S., Kota, A.K., Mabry, J.M. et al. (2013). Superomniphobic surfaces for effective chemical shielding. *Journal of the American Chemical Society* 135 (2): 578–581.
- 44 Zhou, H., Wang, H., Niu, H. et al. (2017). A waterborne coating system for preparing robust, self-healing, superamphiphobic surfaces. *Advanced Functional Materials* 27 (14): 1604261.
- 45 Kang, S.M., Kim, S.M., Kim, H.N. et al. (2012). Robust superomniphobic surfaces with mushroom-like micropillar arrays. *Soft Matter* 8 (33): 8563–8568.
- 46 Jiao, X., Li, M., Yu, X. et al. (2022). Mechanically robust superamphiphobic ceramic coatings with releasable nanoparticle capsules. *Chemical Engineering Journal* 446 (3): 137336.
- 47 Liu, H., Wang, Y., Huang, J. et al. (2018). Bioinspired surfaces with superamphiphobic properties: concepts, synthesis, and applications. *Advanced Functional Materials* 28 (19): 1707415.
- 48 Shome, A., Das, A., Borbora, A. et al. (2022). Role of chemistry in bio-inspired liquid wettability. *Chemical Society Reviews* 51 (13): 5452–5497.
- 49 Si, W. and Guo, Z. (2022). Enhancing the lifespan and durability of superamphiphobic surfaces for potential industrial applications: a review. *Advances in Colloid and Interface Science* 310: 102797.
- 50 Yong, J., Chen, F., Yang, Q. et al. (2017). Superoleophobic surfaces. *Chemical Society Reviews* 46 (14): 4168–4217.
- 51 Tuteja, A., Choi, W., Ma, M. et al. (2007). Designing superoleophobic surfaces. *Science* 318 (5856): 1618–1622.
- 52 Kang, S.M. and Choi, J.S. (2020). Selective Liquid Sliding Surfaces with Springtail-Inspired Concave Mushroom-Like Micropillar Arrays. *Small* 16 (3): 1904612.
- 53 Zhang, D., Wu, G., Li, H. et al. (2021). Superamphiphobic surfaces with robust self-cleaning, abrasion resistance and anti-corrosion. *Chemical Engineering Journal* 406: 126753.
- 54 Wang, T., Lv, C., Ji, L. et al. (2020). Designing re-entrant geometry: construction of a superamphiphobic surface with large-sized particles. *ACS Applied Materials and Interfaces* 12 (43): 49155–49164.

- 55 Li, H., Jin, Q., Li, H. et al. (2024). Transparent superamphiphobic material formed by hierarchical nano re-entrant structure. *Advanced Functional Materials* 34 (3): 2309684.
- 56 Cao, L., Hu, H.H., and Gao, D. (2007). Design and fabrication of micro-textures for inducing a superhydrophobic behavior on hydrophilic materials. *Langmuir* 23 (8): 4310–4314.
- 57 Cao, A., Cao, L., and Gao, D. (2007). Fabrication of nonaging superhydrophobic surfaces by packing flowerlike hematite particles. *Applied Physics Letters* 91 (3): 034102.
- 58 Lee, S.E., Kim, H.J., Lee, S.H. et al. (2013). Superamphiphobic surface by nanotransfer molding and isotropic etching. *Langmuir* 29 (25): 8070–8075.
- 59 Wang, F., Li, J.Y., Pi, J. et al. (2021). Superamphiphobic and flame-retardant coatings with high chemical and mechanical robustness. *Chemical Engineering Journal* 421 (2): 127793.
- 60 Wooh, S., Huesmann, H., Tahir, M.N. et al. (2015). Synthesis of mesoporous supraparticles on superamphiphobic surfaces. *Advanced Materials* 27 (45): 7338–7343.
- 61 Li, F., Du, M., and Zheng, Q. (2016). Dopamine/silica nanoparticle assembled, microscale porous structure for versatile superamphiphobic coating. *ACS Nano* 10 (2): 2910–2921.
- 62 Feng, Y., Peng, C., Hu, J. et al. (2018). Robust wear and pH endurance achieved on snake-shaped silica hybrid nanowire self-woven superamphiphobic membranes with layer-stacked porous 3D networks. *Journal of Materials Chemistry A* 6 (29): 14262–14271.
- 63 Cao, Y., Salvini, A., and Camaiti, M. (2021). One-step fabrication of robust and durable superamphiphobic, self-cleaning surface for outdoor and in situ application on building substrates. *Journal of Colloid and Interface Science* 591: 239–252.

